Materials Science Forum Vols. 408-412 (2002) pp. 323-328

Modeling Texture and Void Evolution in Polycrystals

Ricardo A. Lebensohn[1,2], Carlos N. Tomé[1] and Paul J. Maudlin[1]

[1] Los Alamos National Laboratory, Los Alamos, NM 87545, USA

[2] Instituto de Física Rosario, 27 de Febrero 210 Bis, 2000 Rosario, Argentina

Keywords: Anisotropy, Crystallographic and Morphologic Textures, Dilatational Plasticity, Polycrystal, Porosity, Viscoplastic Self-Consistent Model, Voids

Abstract. In this work we consider the presence of voids of anisotropic shape inside polycrystals submitted to large strain deformation. For this purpose, the originally incompressible viscoplastic selfconsistent (VPSC) formulation has been extended to deal with compressible polycrystals. In doing this, both the deviatoric and the spherical components of strain-rate and stress are accounted for. As a consequence, the extended model provides a relationship between the void growth rate and the hydrostatic pressure allowing porosity evolution. The formulation is validated by comparison with the classical Gurson model formulated for rate-independent isotropic media and spherical voids. This compressible VPSC (CVPSC) model is used to study the coupling between texture, void shape, crystal symmetry and the effect of triaxiality on void growth.

Introduction

The evolution of porosity is of relevance for assessing damage during both quasi-static and high-strain-rate deformation of metallic aggregates [1]. The Gurson criterion [2], which provides a constitutive description of yield stress and porosity evolution, is widely used in simulations of metal deformation. The Gurson model is based on a number of simple assumptions: an effective stress dependence, spherical voids, and rate independence. Such assumptions do not adequately represent many situations in which the anisotropy associated with void shape and material behavior and/or rate effects may play a role. As a consequence, extensions of the Gurson model have been proposed to address some of these issues (e.g: void shape [3,4], matrix anisotropy [5], rate-sensitivity [6]). On the other hand, Ponte Castañeda and coworkers (e.g.: [7]) developed formulations based on variational principles to predict the behavior of porous rate-sensitive materials with isotropic phases, taking into account the anisotropy induced by void shape evolution. In this work we present a 3D viscoplastic selfconsistent (VPSC) model for polycrystal with prexisiting voids, which allows consideration of the full anisotropy associated with mophologic evolution of voids and grains and with crystallographic texture development in the aggregate, as well as rate effects. With an appropriate choice of the local linearized behavior in the grains, this model reproduces Gurson's results for the case of low rate-sensitivity isotropic aggregates with spherical voids. In addition, it accounts for the effect of porosity and texture evolution on the mechanical response of the polycrystal.

Our formulation is a generalization of the tangent incompressible fully anisotropic VPSC formulation developed by Lebensohn and Tomé [8]. This model treats each grain as a viscoplastic ellipsoidal inclusion embedded in a Homogeneous Effective Medium (HEM). Both, the inclusion and the HEM are anisotropic and incompressible. As a consequence, the model was formulated in the deviatoric 5-dim space. In the present extension, cavities are also assumed to be ellipsoidal inclusions, but the assumption of incompressibility does not apply neither to the pores nor to the HEM (the inclusions representing grains, however, remain incompressible). Dilatation and hydrostatic pressure have to be accounted for and represent now the sixth dimension of the problem.

In next section we present a compact description of the formulation and its assumptions while in the following we illustrate some of the capabilities of the model, first by comparison with Gurson

and then with results on the interplay between texture and porosity evolution in fcc and hcp polycrystals with different initial void morphologies and/or crystallographic textures.

Model

Compressible VPSC formulation (CVPSC). The deviatoric part of the constitutive behavior of the material at local level is described by means of the non-linear rate-sensitivity equation:

$$\dot{\varepsilon}'_{ij}(\bar{x}) = \dot{\gamma}_o \sum_s m^s_{ij} \left(\frac{m^s_{kl} : \sigma'_{kl}(\bar{x})}{\tau^s} \right)^n \tag{1}$$

where $\dot{\varepsilon}'(\bar{x})$ and $\sigma'(\bar{x})$ are the deviatoric strain-rate and stress fields; m^s_{ij} and τ^s are the Schmid tensor and the threshold stress of slip (s); $\dot{\gamma}_o$ is a normalization factor and n is the rate-sensitivity exponent. Linearizing equation (1) inside the domain of a grain and adding the spherical local relation gives:

$$\left| \begin{array}{l} \dot{\varepsilon}'_{ij} = M_{ijkl}\ \sigma'_{kl} + \dot{\varepsilon}'^{o}_{ij} \\ \dot{\varepsilon}_{kk} = p / K \end{array} \right. \tag{2}$$

where $\dot{\varepsilon}'$ and $\dot{\sigma}'$ are the average local quantities in the grains; M_{ijkl} and $\dot{\varepsilon}'^{o}_{ij}$ are the local compliance and the back extrapolated term and $\dot{\varepsilon}_{kk}$, p and K are average local dilatation-rate, pressure and viscoplastic bulk modulus, respectively. M_{ijkl} and $\dot{\varepsilon}'^{o}_{ij}$ can be chosen differently. The best choice of them for the case of voided polycrystals is discussed later in this section. Performing homogenization consists in assuming a constitutive relation analogous to (2) at polycrystal level:

$$\left| \begin{array}{l} \dot{E}'_{ij} = \overline{M}_{ijkl}\ \Sigma'_{kl} + \dot{E}'^{o}_{ij} \\ \dot{E}_{kk} = P / \overline{K} \end{array} \right. \tag{3}$$

where, by comparison with (2), the meaning of the macroscopic state variables and moduli becomes aparent. Using the equivalent inclusion method [9] the local (heterogeneous) constitutive behavior can be rewritten in terms of the (homogeneous) macroscopic moduli as:

$$\left| \begin{array}{l} \dot{\varepsilon}'_{ij} = \overline{M}_{ijkl}\ \sigma'_{kl} + \dot{E}'^{o}_{ij} + \dot{\varepsilon}^{*}_{ij} \\ \dot{\varepsilon}_{kk} = p / \overline{K} + \dot{\varepsilon}^{\#} \end{array} \right. \tag{4}$$

where $\dot{\varepsilon}^{*}_{ij}$ and $\dot{\varepsilon}^{\#}$ are the deviatoric eigen-strain-rate and a newly defined eigen-dilatation-rate, respectively. Rearranging and subtracting (3) from (4) gives:

$$\left| \begin{array}{l} \tilde{\sigma}'_{ij} = \overline{L}_{ijkl} \left(\tilde{\dot{\varepsilon}}'_{kl} - \dot{\varepsilon}^{*}_{kl} \right) \\ \tilde{p} = \overline{K} \left(\tilde{\dot{\varepsilon}}_{kk} - \dot{\varepsilon}^{\#} \right) \end{array} \right.$$

where the "~" quantities are local deviations from macroscopic values and $\overline{L}_{ijkl} = \overline{M}^{-1}_{ijkl}$. Using the equilibrium condition: $\sigma_{ij,j} = \tilde{\sigma}_{ij,j} = \tilde{\sigma}'_{ij,j} - \tilde{p}_{,i}$ and having in mind the relation between strain-rate and velocity-gradient, i.e.: $\tilde{\dot{\varepsilon}}_{ij} = \frac{1}{2}\left(\tilde{u}_{i,j} + \tilde{u}_{j,i}\right)$, gives:

$$\left| \begin{array}{l} \overline{L}_{ijkl}\ \tilde{u}_{k,lj} + \tilde{p}_{,i} + f_i = 0 \\ \overline{K}\ \tilde{u}_{k,k} - \tilde{p} + F = 0 \end{array} \right. \tag{6}$$

where the heterogeneity terms explicitly are: $f_i = -\overline{L}_{ijkl}\dot{\varepsilon}^*_{kl,j}$ and $F = -\overline{K}\dot{\varepsilon}^{\#}$. Equation (6) represents a system of 4 differential equations with 4 unknowns (3 components of the deviation in velocity $\tilde{u}_i$ and one deviation in hydrostatic pressure $\tilde{p}$). After solving these differential equations using Green functions and Fourier transforms (described elsewhere [10]) we obtain:

$$\begin{cases} \tilde{\dot{\varepsilon}}'_{ij} = S_{ijmn}\,\dot{\varepsilon}^*_{mn} + \beta_{ij}\,\tilde{\dot{\varepsilon}}_{kk} \\ \tilde{\dot{\varepsilon}}_{kk} = S_{kkmn}\,\dot{\varepsilon}^*_{mn} + \Psi\,\dot{\varepsilon}^{\#} \end{cases}$$

where S_{ijkl} is the fourth order viscoplastic deviatoric Eshelby tensor, $\Psi = S^s_{kk}$ (Ψ and S^s_{ij} are the newly defined viscoplastic spherical Eshelby factor and tensor, respectively) and $\beta_{ij} = S^s_{ij}/\Psi - \frac{1}{3}\delta_{ij}$ is a tensor that vanishes if the medium is isotropic. Inverting (7) the eigen-strain-rates are obtained:

$$\begin{cases} \dot{\varepsilon}^*_{ij} = S^{-1}_{ijmn}\,\tilde{\dot{\varepsilon}}'_{mn} - S^{-1}_{ijmn}\,\beta_{mn}\,\tilde{\dot{\varepsilon}}_{kk} \\ \dot{\varepsilon}^{\#} = \tilde{\dot{\varepsilon}}_{kk}/\Psi \end{cases}$$

Replacing (8) in (5) we obtain the interaction equations:

$$\begin{cases} \tilde{\dot{\varepsilon}}'_{ij} = -\tilde{M}_{ijkl}\,\tilde{\sigma}'_{kl} - \tilde{\beta}_{kl} \\ \tilde{\dot{\varepsilon}}_{kk} = -\tilde{p}/\tilde{K} \end{cases}$$

where $\tilde{\mathbf{M}} = (\mathbf{I}-\mathbf{S}):\mathbf{S}^{-1}:\overline{\mathbf{M}}$; $\tilde{\boldsymbol{\beta}} = -\mathbf{S}^{-1}:\boldsymbol{\beta}\,\tilde{\dot{\varepsilon}}_{kk}$ and $\tilde{K} = (1-\Psi)\Psi^{-1}\overline{K}$. Replacing the constitutive relations (2) and (3) in (9) gives the following self-consistent equations for the macroscopic moduli:

$$\overline{\mathbf{M}} = \frac{n^{eff}}{n}\langle\mathbf{B}\rangle^{-1}:\langle\mathbf{M}:\mathbf{B}\rangle \tag{10}$$

$$\dot{\mathbf{E}}'^{\mathbf{o}} = \langle\mathbf{M}:\boldsymbol{\Phi}+\dot{\boldsymbol{\varepsilon}}'^{\mathbf{o}}\rangle - \langle\mathbf{M}:\mathbf{B}\rangle:\langle\mathbf{B}\rangle^{-1}:\langle\boldsymbol{\Phi}\rangle \tag{11}$$

$$\overline{K} = \frac{1-\phi}{\Psi_v}\,\frac{1-\Psi_g}{\phi}\,\overline{K} \tag{12}$$

where <.> indicates spatial average; n^{eff} is an interaction parameter (typically 10); the localization tensors are functions of the local and macroscopic moduli, i.e.: $\mathbf{B} = (\mathbf{M}+\tilde{\mathbf{M}})^{-1}:(\overline{\mathbf{M}}+\tilde{\mathbf{M}})$ and $\boldsymbol{\Phi} = (\mathbf{M}+\tilde{\mathbf{M}})^{-1}:(\dot{\boldsymbol{\varepsilon}}'^{\mathbf{o}} - \dot{\mathbf{E}}'^{\mathbf{o}} + \tilde{\boldsymbol{\beta}})$; Ψ_g and Ψ_v are the Eshelby factors of grains and voids and ϕ is the porosity. Equations (10-12) are fix-point equations that allow obtaining improved estimates of the macroscopic moduli $\overline{\mathbf{M}}, \dot{\mathbf{E}}'^{\mathbf{o}}$ and $\overline{K}$. Once $\overline{K}$ is adjusted, the macroscopic dilatation-rate is given by: $\dot{E}_{kk} = P/\overline{K}$ and the porosity-rate can be calculated by means of the well-known kinematic relation:

$$\dot{\phi} = (1-\phi)\dot{E}_{kk}$$

Local linearization for voided polycrystals. As stated earlier, the deviatoric local constitutive behavior (1) can be linearized in different ways. The macroscopic response resulting of the selfconsistent formulation will eventually depend on the choice made for that local linearization.

For instance, if the back-extrapolated term $\dot{\varepsilon}'^{o}_{ij}$ is a priori set to zero, the resulting model is a secant one, which has been proved to be in general too stiff, leading to close-to-upper-bound result. On the other hand, if $M_{ijkl} = \partial\dot{\varepsilon}'_{ij}(\sigma')/\partial\sigma'_{kl}$, the model is tangent, a less stiff approach. However, as pointed out by Ponte Castañeda [11] and proved numerically by the authors [10], any homogenization scheme whose local linearization depends only on the average of local states in the phases (or grains) fails in reproducing Gurson's results at high triaxialities, leading to completely rigid response in the pure hydrostatic limit. This result is connected to the high deformation gradients that physically appear inside the phases (or grains), in the vicinities of a void, when high hydrostatic pressure is applied to the aggregate. These strong gradients make the effective response of the phases (or grains) softer than the one that would be obtain by linearization using just the average local states (first order moments). In fact, Suquet [12] showed that estimating the magnitudes of the intraphase (or intragranular) fluctuations (second order moments) and linearizing the local behavior in terms of them, rather than just using the average states, softens the predicted effective behavior of the aggregate. For these reasons, a good matching between the present theory (in its isotropic and rate-insensitive limit) and the Gurson model at high triaxialities requires formulating a supertangent formulation by defining the local compliance as one that fulfills:

$$M_{ijkl}\left(\hat{\sigma}'_{kl} - \sigma'_{kl}\right) = \left(\hat{\dot{\varepsilon}}'_{ij} - \dot{\varepsilon}'_{ij}\right)$$

with:

$$\hat{\sigma}'_{kl} = \left(1 + \alpha(T)T\right)\sigma'_{kl}$$

where T is the triaxiality: $T = \left|P/\Sigma_{eq}\right|$ and, for $n^{eff} = 10$, $\alpha(T) = 0.34 - 0.19\exp(-(T-2)/2)$ is an ad-hoc parameter whose dependence with T has been adjusted to match the CVPSC predictions, in its isotropic and rate-insensitive limit, with Gurson's results. Defined in this way, the local tensors $\hat{\sigma}'_{kl}$ are evidently related with second order stress moments but, rather than estimate them directly, we make use of the ad-hoc parameter $\alpha(T)$ and of the Gurson model to tune the value of α for different triaxialities. Details of the adjustment of $\alpha(T)$ are discussed elsewhere [10].

Results

The supertangent CVPSC model is validated by comparison with the classical Gurson formulation. In doing this, all the anisotropic features of the CVPSC model were switched off and a viscoplastic exponent n=50 was used. Fig. 1 shows the porosity evolution of an isotropic material (or a random fcc polycrystal, (111)<110> slip, 500 orientations) containing spherical voids when deformed in tension, for different triaxialities, as predicted by the Gurson and CVPSC models. In all cases the initial porosity was set to $3\text{x}10^{-4}$. For triaxialities 1/3 and 1 the total longitudinal strain reached a value of 1. In the cases of higher triaxialities, the longitudinal strain was limited by the Carroll-Holt condition [13] that gives a threshold porosity above which the deformation proceeds in a pure hydrostatic condition. The CVPSC code converges even close to the numerically demanding Carroll-Holt limit.

In order to isolate the effects of void morphology from the full anisotropy evolution due to morphologic and crystallographic texture development, Fig. 2 shows the CVPSC predictions of porosity evolution for the same fcc polycrystal as above, for: a) different initial void morphologies when no texture or morphology evolution were allowed and b) initial spherical voids with evolving texture and morphology, for triaxialities 1/3 and 1. In all cases, the initial porosity is 1% and the

total longitudinal strain is 0.5. It is seen that oblate voids (ellipsoid's ratios 5:5:1) tends to grow faster than prolate ones (ellipsoid's ratios 1:1:5) and that texture evolution favors porosity growth, even if the voids become prolate as deformation proceeds.

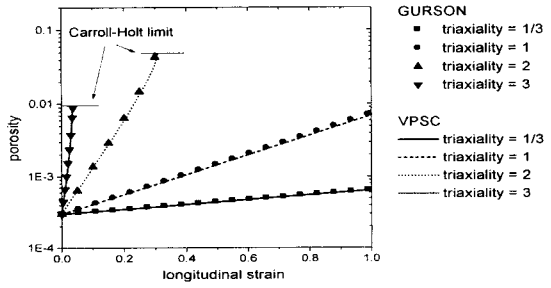

Figure 1: Comparison between Gurson and CVPSC. Porosity evolution in an isotropic material (random polycrystal) with spherical voids deformed in tension, for different triaxialities, predicted with Gurson (symbols) and CVPSC (lines) models. Initial porosity: $3x10^{-4}$. Total longitudinal strain: 1.0, for triaxialities 1/3 and 1. In the cases of triaxialities 2 and 3 the longitudinal strain was limited by Carroll and Holt condition [13]. No texture or morphology evolution was allowed in CVPSC cases.

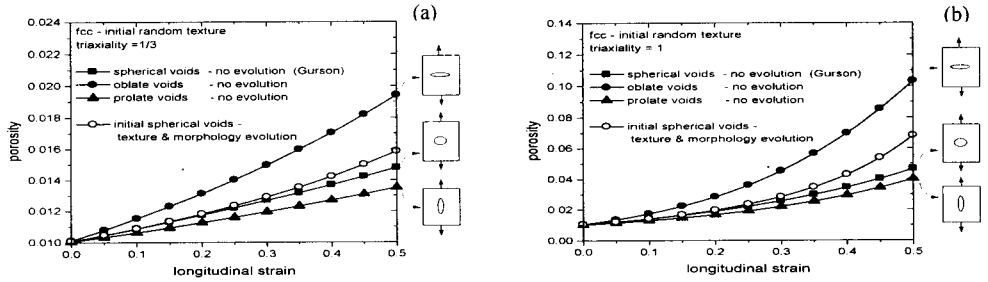

Figure 2: CVPSC predictions of porosity evolution for different void morphologies and no texture or morphology evolution (solid symbols) and for initial spherical voids with evolving texture and morphology (open symbols). Initial porosity: 1%, total longitudinal strain: 0.5. Cases of: a) triaxiality 1/3, b) triaxiality 1.

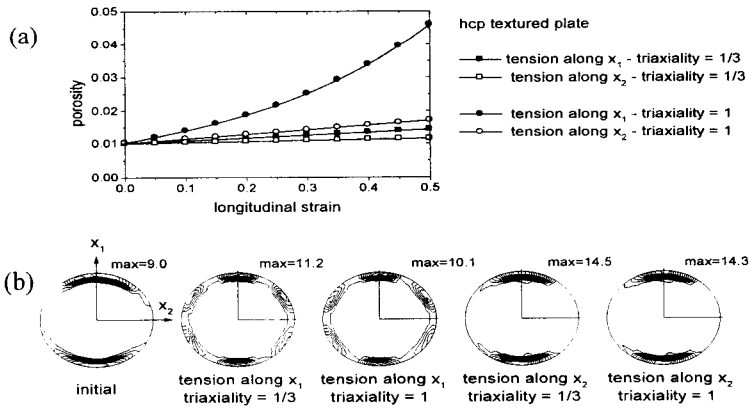

Figure 3: Interplay between texture and porosity. CVPSC predictions of: a) porosity evolution in an initially textured hcp polycrystal, deformed in tension along x_1 and x_2, for triaxialities 1/3 and 1. Initial porosity: 1%. Slip modes: prismatic and basal slip (τ^s =1) and pyramidal <c+a> slip (τ^s =4). Total longitudinal strain: 0.5. b) initial and final (0001) basal poles figures for the four cases shown above.

The next example concerns an hcp aggregate and reveals a strong coupling between texture and porosity evolution. In this case we consider an aggregate of 500 grains with easy basal and prismatic

slip (τs =1) and hard pyramidal <c+a> slip (τs =4), and an initial strong texture consisting of a basal component along the axis x1 (see Fig. 3b). Tension was imposed parallel to the axis x1 or perpendicular to it (along axis x2), triaxialities of 1/3 and 1 were enforced, and an initial concentration ϕ=0.01 of spherical voids was considered. Texture evolution is not very sensitive to triaxiality, and rather depends on the relative orientation of the initial texture and the tensile axis (see Fig. 3b). The porosity evolution, instead, is strongly influenced by the texture, especially at high triaxialities (Fig. 3a). Indeed, the cases of tension along x1 (i.e.: most crystals with their <c>-axis aligned in tensile direction and therefore hard to deform) exhibit a faster void growth than the cases of tension along x2, which final porosities for triaxialities 1/3 and 1 do not differ substantially.

Conclusions

We propose a compressible VPSC polycrystal model (CVPSC) which accounts for porosity and texture, and their evolution, during plastic forming. The model is tuned to give the same response as Gurson when the material has low rate-sensitivity, is isotropic and the cavities are spherical. Such tunning is done through a single parameter, function of triaxiality. A direct connection exists between this parameter and the second order stress moment associated with the stress gradients in the grains, required to accommodate locally the deformation of the voids. Such second order moment dependence was formally introduced by Ponte Castañeda [11,12] in his variational formalisms. We may say that, in much the same way as VPSC represents an improvement over the sotropic Von Mises plastic formulation, CVPSC represents an improvement over the simple isotropic Gurson formulation.

The main results shown in this work are: a) the void shape has a major effect on porosity evolution, oblate voids tends to grow faster than prolate voids under tensile stress; b) Porosity evolution does not affect substantially texture evolution by comparison with an aggregate without voids deformed to the same strain; c) texture changes substantially the porosity evolution in the case of a textured and highly anisotropic hexagonal aggregate tested along and across the main texture component.

Acknowledgments.

The authors wish to thank Prof. P. Ponte Castañeda for fruitful discussions.

References

[1] J.N Johnson and F.L. Addessio: J. Appl. Phys. 74 (1988), 1640.

[2] A.L. Gurson: J. Eng. Mater. Technol. 99 (1977), 2.

[3] V. Tveergard: Int. J. Fracture 17 (1981), 389.

[4] M. Golaganu, J.B. Leblond and J. Devaux: J. Mech. Phys. Solids 41 (1993), 1723.

[5] B. Chen, Z.C Xia, S.R. McEwen, S.C. Tang and Y. Huang: in *Multiscale Deformation and Fracture in Materials and Structures.* (Kluwer Academic Publishers, Dordrecht, 2000), pp. 17-30.

[6] B. Chen, Y. Huang, C.Liu, P.D. Wu and S.R. McEwen: Eng. Fract. Mech., submitted.

[7] M. Kailasam, P. Ponte Castañeda and J.R.Willis: Phil. Trans. R. Soc. Lond. A. 355 (1997) 1835.

[8] R.A. Lebensohn and C.N. Tomé: Acta Metall. Mater. 41 (1993) 2611.

[9] T. Mura: *Micromechanics of Defects in Solid*s (Martinus-Nijhoff, Dodrecht, 1988).

[10] R.A. Lebensohn, C.N. Tomé and P.J. Maudlin, to be published.

[11] P. Ponte Castañeda: J. Mech. Phys. Solids 50 (2002), 737

[12] P. Suquet: C.R. Acad Sci. Paris IIb 320 (1995) 563.

[13] M.M. Carroll and A.C. Holt: J. Appl. Phys. 43 (1972) 1626.